Transitions between Patterns in Thermal Convection

Eberhard Bodenschatz,[1] John R. de Bruyn,[2] Guenter Ahlers,[1] and David S. Cannell[1]
[1]*Department of Physics and Center for Nonlinear Science, University of California, Santa Barbara, Santa Barbara, California 93106*
[2]*Memorial University of Newfoundland, St. John's, Newfoundland, Canada A1B 3X7*
(Received 5 August 1991)

We present experimental studies of the transitions between conduction, hexagons, and rolls in non-Boussinesq convection of gaseous CO_2 in a cylindrical cell of radius-to-height ratio 86. Except for the transition from conduction to hexagons, transitions occur when the two states involved have nearly the same value of a generalized potential rather than at the stability limits. Conduction gives way to hexagons via the propagation of a front connecting the two states, while the transitions between hexagons and rolls are facilitated at the cell walls which appear to nucleate the minority state.

PACS numbers: 47.20.Bp, 47.25.Qv

Transitions and competition among patterns of different symmetries are fundamental problems in nonequilibrium systems. Convection in a horizontal fluid layer subject to a vertical temperature gradient is particularly well suited to their study. Near the onset of convection, roll, hexagonal, triangular, and square patterns can exist, and bistability and tristability can occur depending on the particular experimental situation [1].

An example amenable to detailed experimental and theoretical study is convection of a fluid with temperature-dependent properties, known as non-Oberbeck-Boussinesq (non-OB) convection. Bistability and hysteretic transitions between conduction and hexagons and between hexagons and rolls are predicted theoretically [2]. While the latter have been investigated experimentally to some extent [1,3–6], the hysteresis in the transition between conduction and hexagons has been studied [3] only without flow visualization, and in a parameter range where the theory is only qualitative. In a recent experiment [4–6] with a cylindrical cell of aspect ratio $\Gamma=20$ (radius/height), the hysteretic transition between hexagons and rolls was dominated by competition between the two patterns. Quantitative agreement with theory [2] was not found; incorporating finite-size effects did not resolve the discrepancies [6].

In this Letter, we report high-resolution experimental results for non-OB convection in a much larger cylindrical cell ($\Gamma=86$) than had been used previously. Near onset, we measured the size of the small hysteresis loop between conduction and hexagons. Above onset, we observed a defect-free hexagonal pattern containing approximately 5000 convection cells. We found that the transition from perfect hexagons to rolls and vice versa is only very weakly hysteretic. It occurred when the two states had nearly the same value of a generalized potential derived from amplitude equations [2,7–9], instead of being triggered by instabilities. Within the stability regime of rolls we observed stable rotating spirals. We did not expect the latter phenomenon, and it is not understood theoretically.

The experiment was performed in a cylindrical cell of diameter $D=8.941\pm0.001$ cm and height $d=0.0520\pm0.0005$ cm. The bottom of the cell was a 0.64-cm-thick silver disk with a flat mirror surface. The top was a flat 0.32-cm-thick sapphire. The cell height varied less than ±0.5 μm over the central 80% of the cell area, as measured interferometrically. The lateral wall was made of Macor [10,11]. The cell was horizontal within $\pm8\times10^{-5}$ rad and filled with CO_2 at a pressure of 21.8 ± 0.1 bars controlled to ±0.1 mbar. The vertical thermal diffusion time $\tau_v=d^2/\kappa\approx0.8$ s (κ is the thermal diffusivity). The bottom-plate temperature was regulated to ±0.2 mK. The top-plate temperature was held constant at 12.84 ± 0.05 °C and regulated to ±5 mK by circulating water. We found the critical temperature difference to be $\Delta T_c=29.026\pm0.005$ K; the theoretical value estimated from the Rayleigh number R at its criti-

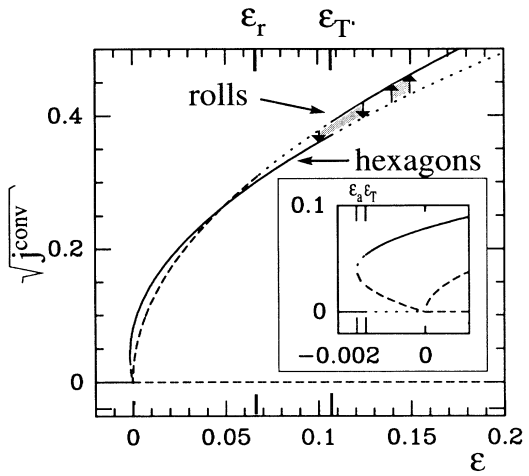

FIG. 1. Convective heat current vs ε for our experimental conditions. The inset is the region near onset. Absolutely stable solutions are shown as solid lines, metastable solutions as dotted lines, and unstable solutions as dashed lines. The thermodynamic thresholds ε_T and $\varepsilon_{T'}$, to be defined in the text, are located where the dotted and solid lines join. The shadings and the arrows indicate the experimentally observed transition regions.

cal value R_c [12], the height, and the fluid properties is 28.55 ± 1.0 K. We resolved steps in $\varepsilon = R/R_c - 1$ as small as 3×10^{-5} and visualized [13] patterns with the shadowgraph technique.

Stability analysis for a non-OB fluid [2] leads to the diagram of Fig. 1, which shows the square root of the convective heat current j^{conv} vs ε. At onset, convection starts via a subcritical bifurcation to hexagons. For $\varepsilon_a \leq \varepsilon \leq 0$, both hexagons and conduction are stable. For $0 \leq \varepsilon \leq \varepsilon_r$, only hexagons are stable, while for $\varepsilon_r \leq \varepsilon \leq \varepsilon_b$ both hexagons and rolls are stable. For $\varepsilon \geq \varepsilon_b$, only rolls are stable. Since the midplane temperature changed with the applied ΔT, the fluid properties varied [14]. Consequently, the predicted thresholds ε_a, ε_r, etc., also varied as shown in Fig. 2. It is clear that ε_b, where hexagons lose stability to rolls, was not approached in this experiment.

On increasing ΔT quasistatically, we observed a transition from conduction to hexagons in a small patch at a preferred site. Figure 3(a) shows a shadowgraph picture of a part of the convection cell immediately after the appearance of the hexagons. Dark corresponds to warm upflow and bright to cold downflow. As shown, the hexagonal patch grew by a six-faceted, moving front. The three independent roll states, which in superposition give the hexagonal structure, are observable. After about $750\tau_v$ the front came to a halt and the stable pattern shown in Fig. 3(b) was reached [15]. We can explain the final size by a temperature gradient [11] near the side, and by slight variations in the cell height, since $R \propto d^3 \Delta T$. On decreasing ΔT quasistatically, the patch of hexagons shrunk to the pattern of Fig. 3(c), which disappeared after reducing ε further by 3×10^{-5}. The orientation of the hexagonal pattern appearing at onset changed from one experimental run to the next.

Near onset the flow can be described by three coupled amplitude equations [2,7–9]. The complex amplitudes A_k, A_l, and A_m describe slow variations of modulus and phase of periodic roll solutions [2] with wave vectors $\mathbf{q}_k, \mathbf{q}_l, \mathbf{q}_m$ with $\sum \mathbf{q}_i = 0$ $(i = k,l,m)$ and $|\mathbf{q}_i| = q_c$. For a homogeneous pattern with $|\mathbf{q}_i| = q_c$ the amplitudes are real and the equations read as

$$\dot{A}_k = \varepsilon A_k - a A_l A_m - b(A_l^2 + A_m^2) A_k - A_k^3 , \qquad (1)$$

where the other two equations are obtained by circular permutation of k,l,m. Expressions for a and b, and the relationship of the A_i to the convective heat current j^{conv}, are given in Ref. [16]. The parameter a depends on the extent to which the fluid departs from the Oberbeck-Boussinesq approximation, for which $a = 0$. There are three stationary solutions [2,7–9]: conduction ($A_k = A_l = A_m = 0$), hexagons ($A_k = A_l = A_m = A_{\text{hex}}$), and rolls

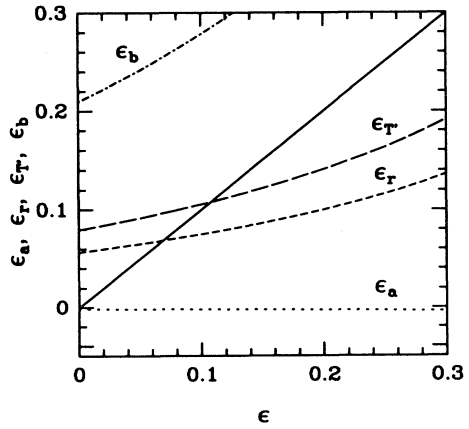

FIG. 2. Instabilities and thermodynamic thresholds vs ε. The solid line gives the experimental path. The thermodynamic threshold ε_T is given by $\frac{8}{9}\varepsilon_a$.

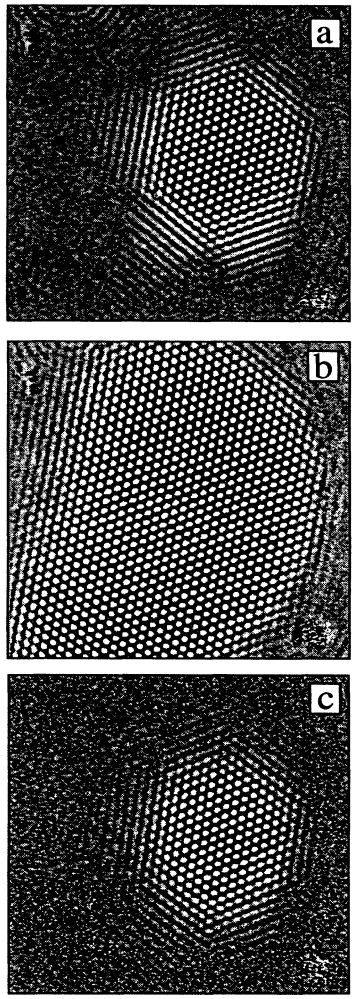

FIG. 3. (a) Hexagons appeared at $\varepsilon = 0$ and spread. (b) Stable pattern at $\varepsilon = 0$ after transients had died out. (c) Stable pattern at $\varepsilon = -1.92 \times 10^{-3} \cong \varepsilon_T$. The circular pattern in the upper left-hand corner was caused by a dust particle. The spot at the lower right-hand corner was caused by lower reflectivity of the bottom plate. Neither inhomogeneity seemed to influence the experimental observations.

($A_k = A_{\text{roll}}$, $A_l = A_m = 0$). The stability thresholds [17] ε_a, ε_r, and ε_b were discussed above and shown in Fig. 2. For $a > 0$ ($a < 0$), only hexagons with upflow (downflow) in the center are stable. For gases $a < 0$, and downflow hexagons are chosen.

Equations (1) have a generalized potential [2,7–9] Φ, such that $\dot{A}_i = -\partial\Phi/\partial A_i$. An absolutely stable state corresponds to the global minimum of Φ, while metastable states correspond to local minima. Any dynamics of the pattern will decrease the potential. Its existence ensures that two stable phases can coexist only when they have the same value for Φ. We define the value of ε at which this occurs as ε_T for coexistence of conduction and hexagons, and as $\varepsilon_{T'}$ for coexistence of hexagons and rolls. As shown in Fig. 1, for $\varepsilon < \varepsilon_T < 0$, conduction, for $\varepsilon_T < \varepsilon < \varepsilon_{T'}$, hexagons, and, for $\varepsilon > \varepsilon_{T'}$, rolls are the absolutely stable states [9,18]. For values of ε other than ε_T and $\varepsilon_{T'}$, the front between the two states will move so that the state with the lower potential spreads [9]. Thus we can explain the experimental observations shown in Fig. 3 by the cell filling with hexagons until the spatially varying ε reaches ε_T. On decreasing ε the hexagons disappear when $\varepsilon < \varepsilon_T$ throughout the cell [Fig. 3(c)].

Experimentally, we found $\varepsilon_T = -(2.0 \pm 0.1) \times 10^{-3}$ and $\varepsilon_a = -(2.3 \pm 0.1) \times 10^{-3}$. The theoretical value for ε_a is -1.65×10^{-3}; the error due to uncertainties in the height and material properties is only $\pm 5 \times 10^{-5}$. Possible explanations for the discrepancies might be found in the breakdown of the perturbation expansion [2] or the spatial inhomogeneity of the cell. The wave number q in units of d^{-1} was 3.14 ± 0.07, in good agreement with the theoretical result [2] $q_c = 3.117$.

On increasing ε, hexagons filled the cell [11] at $\varepsilon \cong 0.02$, as shown in Fig. 4. The circular rolls close to the sidewalls are due to static sidewall forcing [11]. Even on jumping to finite ε, initial dislocations and grain boundaries annihilated and a well-ordered pattern was reached after $\sim 15\Gamma^2 t_v$.

In this experiment it was not possible to reach ε_b, the threshold for the instability of hexagons to rolls. Nevertheless, we observed a transition from hexagons to rolls and vice versa. When, starting with a defect-free hexagonal lattice, we increased ε quasistatically to values close to $\varepsilon_{T'}$, we observed time dependence in a belt of width $\sim 20d$ adjacent to the sidewalls. The rest of the pattern was defect-free. The wave number decreased as ε increased, and close to the transition $q = 3.07 \pm 0.07$. At the transition, rolls appeared in the time-dependent belt and invaded the rest of the cell. We observed a long transient $\sim 20\Gamma^2 t_v$, where rolls and hexagons competed; rolls had a tendency to bend and form local patches of spiral patterns. Eventually, the pattern ordered into a rotating n-armed spiral terminating in n dislocations, such as the two-armed spiral shown in Fig. 5. We observed cases where a spiral extended to the cell boundary, and others where it was surrounded by concentric rolls. The sense of rotation of the spirals was such that the resulting waves propagated out from the spiral core. While the spiral was rotating, the dislocations rotated on circles at the same frequency and annihilated the spiral waves. We observed stable spirals of left and right handedness and with values of n from 0 to 13. The period of rotation was always similar to that given for the two-armed spiral in Fig. 2, but no detailed investigation was done. The wave numbers of the rolls were close to that of the hexagons before the transition.

On decreasing ε quasistatically, a transition back to hexagons occurred. They appeared in small spots at the

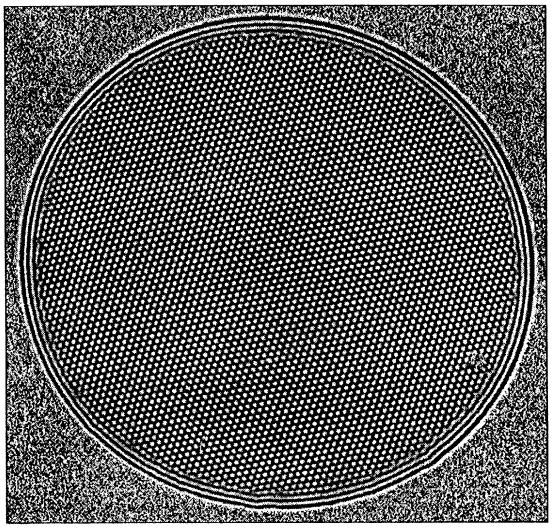

FIG. 4. Shadowgraph picture of hexagons at $\varepsilon = 0.06$. The circular disk is the convection cell. The spot at the lower right of the picture is also seen in Fig. 3.

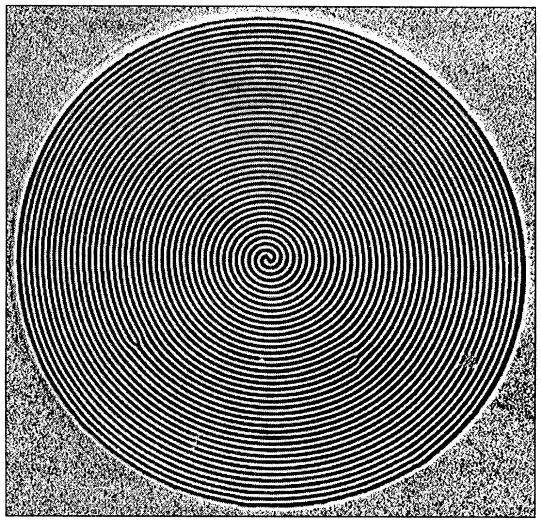

FIG. 5. Two armed spiral at $\varepsilon = 0.15$. The spiral rotates clockwise with a period of $\sim 2400 t_v$.

boundaries and invaded the cell. There was no competition between hexagons and rolls. The rolls quickly disappeared, leaving a very disordered pattern of hexagons, which healed into a defect-free hexagonal lattice after a transient of about $15\Gamma^2 t_v$. The wave number was the same as that of the hexagonal pattern before the transition to rolls.

In Fig. 1 the shaded areas and the arrows indicate the experimentally observed transition regions. We found that the actual transition points and the extent of the hysteresis depended on the size of and the time intervals between steps in ε, with longer time intervals giving a smaller hysteresis loop. The transition regions lie very near $\varepsilon_{T'}$. In analogy with first-order phase transitions, the appearance of the "thermodynamically" preferred phase at the boundaries is reminiscent of heterogeneous nucleation.

The time dependence of the hexagonal pattern near the sidewalls which preceded the breakup of the lattice, the transition to spiral states at slightly higher ε, and the periodically time-dependent spirals cannot be explained by a model like Eq. (1), which has a potential even after inclusion of linear gradient terms [7,9]. An explanation of these nonrelaxational effects will presumably require the inclusion of nonpotential, nonlinear gradient terms [8], and of large-scale flow [19]. It remains to be seen whether stochastic fields [7,20] will also have to be included in order to describe the experimental observations near the thermodynamic thresholds.

We can also comment on the results by Ciliberto, Pampaloni, and Pérez-Garcia [4]. They found a transition region between hexagons and rolls of size $0.03 < \varepsilon < 0.09$, while the instability threshold predicted by theory occurs at $\varepsilon_b = 0.18$. For their conditions, we calculate $\varepsilon_{T'} = 0.07$, which lies within their experimentally observed transition region. Considering our observation of the time-dependent belt, we think that the wide transition region and time dependence found might be due to the smaller aspect ratio used there.

We thank R. M. Clever, P. C. Hohenberg, and M. Tveitereid for fruitful comments and discussions. This work was supported by U.S. Department of Energy Grant No. DE-FG03-87ER13738. E.B. was also supported by the Deutsche Forschungsgemeinschaft and J.B. by NSERC of Canada.

[1] See, for instance, F. H. Busse, in *Mantle Convection,* edited by W. R. Peltier (Gordon and Breach, New York, 1989), and references therein.

[2] F. H. Busse, J. Fluid Mech. **30**, 625 (1967), and references therein. Note that Eq. (3.7) should read $\varphi_{ln} \equiv -\mathbf{k}_l \cdot \mathbf{k}_n / a_c^2$.

[3] R. W. Walden and G. Ahlers, J. Fluid Mech. **109**, 89 (1981).

[4] S. Ciliberto, E. Pampaloni, and C. Pérez-Garcia, Phys. Rev. Lett. **61**, 1198 (1988).

[5] S. Ciliberto, P. Coullet, J. Lega, E. Pampaloni, and C. Pérez-Garcia, Phys. Rev. Lett. **65**, 2370 (1990).

[6] C. Pérez-Garcia, E. Pampaloni, and S. Ciliberto, Europhys. Lett. **12**, 51 (1990). Note that Eq. (3) should read $\varepsilon_s = -a^2/(8b+4c)$.

[7] H. Haken, Rev. Mod. Phys. **47**, 67 (1975).

[8] H. R. Brand, Prog. Theor. Phys. Suppl. **99**, 442 (1989).

[9] See, for example, B. A. Malomed, A. A. Nepomnyashchy, and M. I. Tribelsky, Phys. Rev. A **42**, 7244 (1990), and references therein.

[10] MACOR Machinable Ceramic, Corning Glass Works, New York.

[11] Conduction through the Macor generated a small radial temperature gradient in the sapphire near the wall. By observing the ε dependence of the boundary between conduction and hexagons, we estimate $\Delta\varepsilon = -0.02$ in an annular region of width $10d$. This gradient produced the circular rolls adjacent to the walls (see Ref. [13]), visible in Fig. 4.

[12] To first order in the departures from the OB approximation, as considered in Ref. [2], $R_c = 1708$.

[13] V. Steinberg, G. Ahlers, and D. S. Cannell, Phys. Scr. **32**, 534 (1985).

[14] Approximately, one has $\Delta T_c = 15.88 + 0.443\Delta T$, $\sigma = 0.94 - 0.0016\Delta T$, $\mathcal{P} = -0.64 - 0.0951\Delta T$. Here the σ dependence of the non-OB parameter $\mathcal{P}$ was taken for free-free boundaries.

[15] The hexagons drifted very slowly through the convecting region in a direction and at a rate determined by the cell leveling (typically $\omega t_v = 3 \times 10^{-3}$).

[16] Following Ref. [2]: $a = \mathcal{P}(6/R_c X)^{1/2}$ and $b = Y/X$, with $X = 1.39892 - 0.00944/\sigma + 0.01665/\sigma^2$, $Y = 1.98148 + 0.15349/\sigma + 0.19529/\sigma^2$, and $R_c = 1708$, where $\sigma = \nu/\kappa$ is the Prandtl number and $\mathcal{P}$ is the non-OB parameter defined in Ref. [2]. $j_{\text{conv}} = |A|^2/2XN$, where $N = 1$ and $A = |A_{\text{roll}}|$ for rolls and $N = 3$ and $A = |A_{\text{hex}}|$ for hexagons.

[17] $\varepsilon_a = -a^2/(4+8b)$, $\varepsilon_r = a^2/(1-b)^2$, and $\varepsilon_b = a^2(2+b)/(1-b)^2$.

[18] $\varepsilon_T = \frac{8}{9}\varepsilon_a$ and $\varepsilon_{T'} = aZ + (2b+1)Z^2$, with $Z = ab/D + [a^2b^2/D^2 + a^2/2D]^{1/2}$, and $D = 1 + b - 2b^2$.

[19] E. Siggia and A. Zippelius, Phys. Fluids **26**, 2905 (1983).

[20] See, for example, J. Swift and P. C. Hohenberg, Phys. Rev. A **15**, 319 (1977).

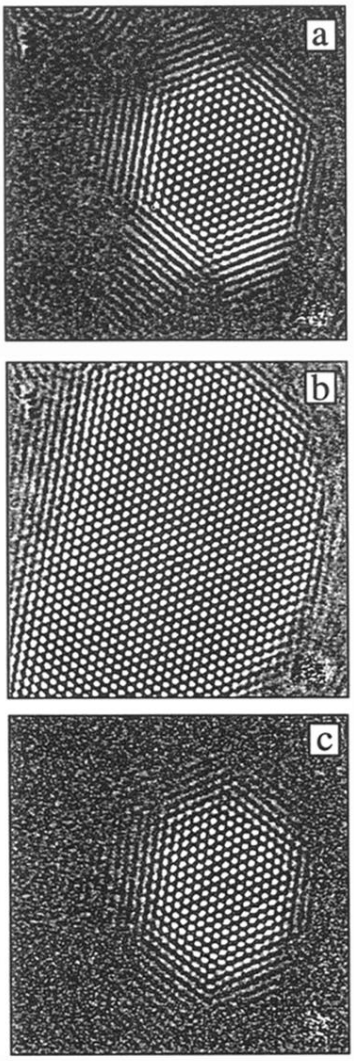

FIG. 3. (a) Hexagons appeared at $\varepsilon=0$ and spread. (b) Stable pattern at $\varepsilon=0$ after transients had died out. (c) Stable pattern at $\varepsilon=-1.92\times10^{-3}\cong\varepsilon_T$. The circular pattern in the upper left-hand corner was caused by a dust particle. The spot at the lower right-hand corner was caused by lower reflectivity of the bottom plate. Neither inhomogeneity seemed to influence the experimental observations.

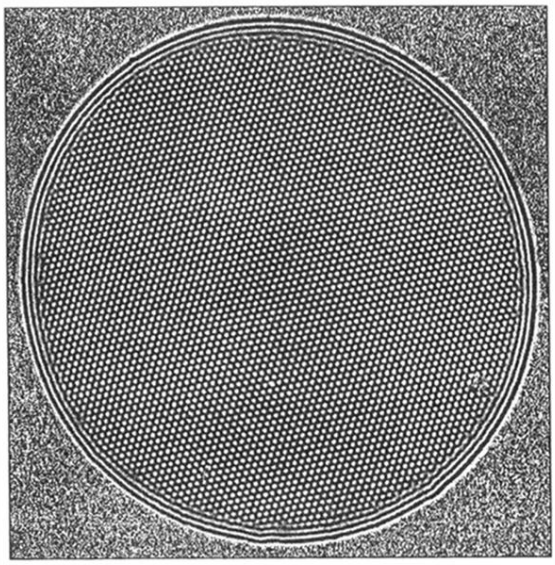

FIG. 4. Shadowgraph picture of hexagons at $\varepsilon=0.06$. The circular disk is the convection cell. The spot at the lower right of the picture is also seen in Fig. 3.

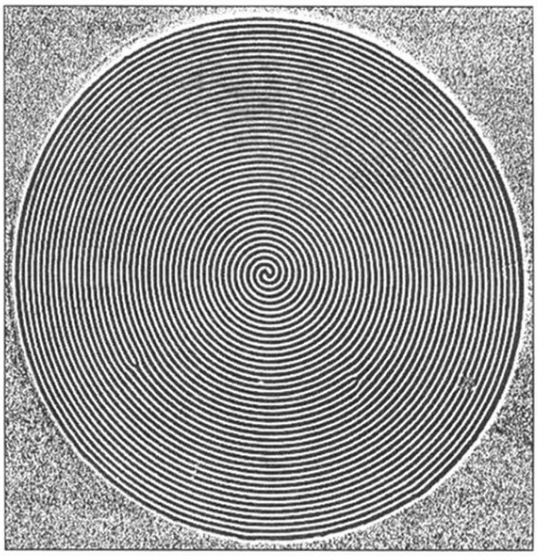

FIG. 5. Two armed spiral at $\varepsilon=0.15$. The spiral rotates clockwise with a period of $\sim 2400 t_r$.